Exchange-correlation energy for the three-dimensional homogeneous electron gas at arbitrary temperature

Ethan W. Brown[*]

Department of Physics, University of Illinois at Urbana-Champaign, 1110 W. Green St., Urbana, Illinois 61801-3080, USA
and Lawrence Livermore National Laboratory, 7000 East Ave, L-415, Livermore, California 94550, USA

Jonathan L. DuBois

Lawrence Livermore National Laboratory, 7000 East Ave, L-415, Livermore, California 94550, USA

Markus Holzmann

LPTMC, UMR 7600 of CNRS, Universit Pierre et Marie Curie, 75005 Paris, France;
Université Grenoble 1/CNRS, LPMMC, UMR 5493, Boîte Postale 166, 38042 Grenoble, France;
and European Theoretical Spectroscopy Facility, Grenoble, France

David M. Ceperley

Department of Physics, University of Illinois at Urbana-Champaign, 1110 W. Green St., Urbana, Illinois 61801-3080, USA

We fit finite-temperature path integral Monte Carlo calculations of the exchange-correlation energy of the 3D finite-temperature homogeneous electron gas in the warm-dense regime [$r_s \equiv (3/4\pi n)^{1/3}a_B^{-1} < 40$ and $\Theta \equiv T/T_F > 0.0625$]. In doing so, we construct a Padé approximant which collapses to Debye-Hückel theory in the high-temperature, low-density limit. Likewise, the zero-temperature limit matches the numerical results of ground-state quantum Monte Carlo, as well as analytical results in the high-density limit.

I. INTRODUCTION

Density functional theory (DFT) is used ubiquitously in computational chemistry and condensed-matter physics.[1,2] Recently there has been intense interest in extending the success of ground-state DFT to finite-temperature systems such as stellar, planetary interiors and other hot dense plasmas.[3–5] However, such attempts have met both fundamental and technical barriers when electrons have significant correlations.

There are two broad approaches to building finite-temperature functionals. In one approach, the exact Mermin finite-T DFT is approximated by smearing the electronic density of states over a Fermi-Dirac distribution.[6] Although a useful approximation, this approach is not exact even in the limit of the exact ground-state exchange functional as the Kohn-Sham orbitals need have no relation to the true excited states.[7] Additionally, as temperature increases, an ever-increasing number of molecular (Kohn-Sham) orbitals is required in order to evaluate the functional. This inevitably results in the DFT calculations becoming computationally intractable at some temperature. A second approach is to use orbital-free density functional theory (OFDFT) where the usual Kohn-Sham orbitals are replaced by explicit density functionals for the kinetic energy and entropy terms.[8,9] However, an *a priori* way to determine such functionals has yet to materialize. Without a reliable benchmark, OFDFT has historically been left to rely on Thomas-Fermi-like approximations which can incur errors an order of magnitude larger than typical DFT errors.[7] Recently generalized gradient approximations have improved OFDFT, introducing higher accuracy orbital-free kinetic energy density functionals for both $0T$ and finite T,[10,11] as well as an exchange-correlation density functional for $0T$.[12] Nevertheless, the field still lacks a high-accuracy,

orbital-free exchange-correlation energy density functional for finite T.

In a recent paper, we provided accurate, first-principles thermodynamic data of the 3D homogeneous electron gas (HEG) throughout the warm-dense regime, making firm connections to both previous semiclassical and ground-state studies.[13] In that work we utilized the restricted path integral Monte Carlo (RPIMC) method.[14–16] Now, we fit this data to a functional form for the exchange-correlation energy which obeys the exact limiting behavior in temperature and density.

II. ASYMPTOTIC LIMITS

A satisfactory fit must match with known asymptotic limits. For the 3D HEG, analytic limits exist at high temperature and low density (the Debye-Hückel limit), and at zero temperature.

In the Debye-Hückel (DH) limit, the quantum-mechanical Fermi-Dirac distribution may be approximated by the classical Boltzmann distribution, i.e., when $\Gamma \equiv 2/(r_s T) \ll 1$, where T is in Rydbergs and r_s is the Wigner-Seitz radius normalized by the Bohr radius. In this regime, the average potential energy per particle is much smaller than the thermal energy per particle, and each electron may be treated with a short-ranged, spherically symmetric, screened interaction.[17] These approximations combined give the excess energy per particle to be $U_{DH} \equiv U - U_0 = -\frac{\sqrt{3}}{2}\Gamma^{3/2}T = -\sqrt{6}r_s^{-3/2}T^{-1/2}$, where U_0 is the energy of an ideal gas (classically) or of a free Fermi gas (quantum mechanically). Classical simulations have numerically extended these results to larger values of Γ.[18,19]

The first-order quantum-mechanical correction to these results is given through the Wigner-Kirkwood expansion in powers of $\hbar$, $U_Q = -\frac{\Gamma^3}{8}T^2 = -r_s^{-3}T^{-1}$. The next order correction as well as the first-order exchange correction have
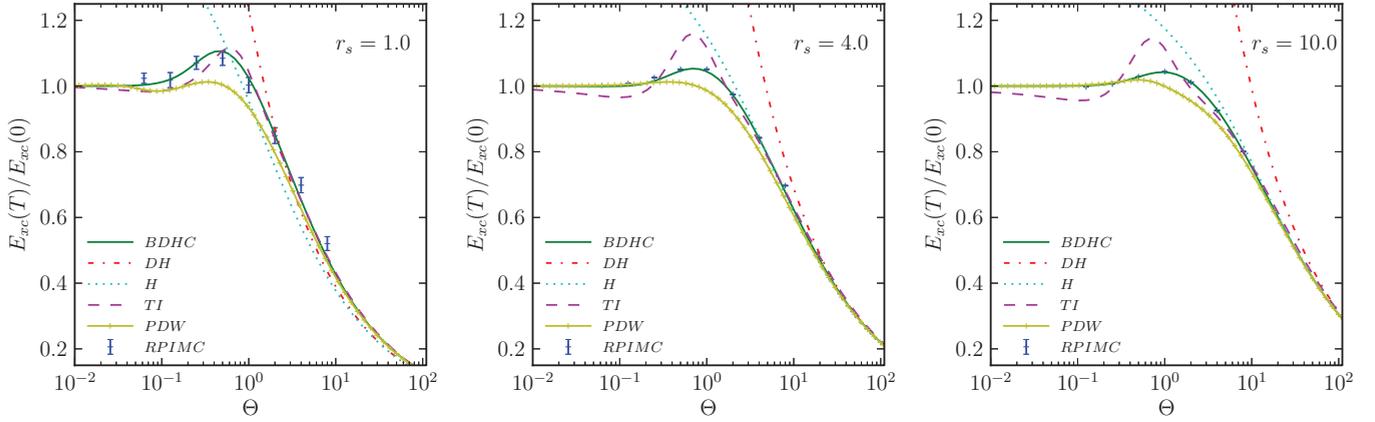
FIG. 1. (Color online) Ratio of the exchange-correlation energy E_{xc} at temperature T to that at $T = 0$ for the unpolarized $\xi = 0$ 3D HEG with $r_s = 1.0$, 4.0, and 10.0 (respectively). Shown are the results from numerical calculations (RPIMC), the present parametrization (BDHC), and several previous parametrizations. The latter include Debye-Hückel (DH), Hansen (H), Tanaka and Ichimaru (TI), and Perrot and Dharma-wardana (PDW), all of which are discussed in the text.

also been calculated explicitly.[20,21] Finally there has been some effort to calculate virial expansions of the excess energy at low density and finite temperature.[22]

At zero temperature, a significant body of numerical and analytical work has defined the exchange-correlation energy at all densities. In the high-density limit ($r_s \ll 1$) the total energy can be expressed as $E = a_1 r_s^{-2} + a_2 r_s^{-1} + a_3 \ln r_s + a_4 + a_5 r_s \ln r_s + a_6 r_s + O(r_s^2 \ln r_s)$. The first two coefficients can be determined through Hartree-Fock theory, with the first being the energy of a free Fermi gas and the second being the Fock exchange energy. Terms a_3 and a_4 were calculated by Gell-Mann and Brueckner[23] using the random phase approximation (RPA). These results were extended by Carr and Maradudin[24] to determine a_5 and a_6. In the low-density limit ($r_s \gg 1$), one expects a body-centered cubic configuration, i.e., the Wigner crystal.[25] This suggests the form $E = A_1 r_s^{-1} + A_2 r_s^{-3/2} + A_3 r_s^{-2} + A_4 r_s^{-5/2} + O(r_s^{-3})$ for the total energy. The first coefficient, the Madelung term, was first calculated by Fuchs.[26] The next three terms, coming from the zero-point harmonic vibration and its associated anharmonic corrections, were determined by Carr *et al.*[27]

High-precision quantum Monte Carlo (QMC) calculations have since spanned these two regimes,[28,29] paving the way for accurate parametrizations which leverage the foregoing limiting forms.[30–32] Such functionals have been integral to the development and expansion of the local density approximation (LDA) of zero-temperature DFT.[33]

III. PRIOR FITS

Several attempts have been made at extending the success of ground-state DFT to finite temperature and this has resulted in the creation of a number of finite-temperature parametrizations of the exchange-correlation energy.[34–37] A basic approach is the RPA, which is accurate in the low-density, high-temperature limit (where it reduces to DH) and the low-temperature, high-density limit, since these are both weakly interacting regimes. Its failure, however, is most apparent in its estimation of the equilibrium, radial distribution function $g(r)$ which becomes unphysically negative for stronger coupling.[37]

Extensions of the RPA into intermediate densities and temperatures have largely focused on constructing
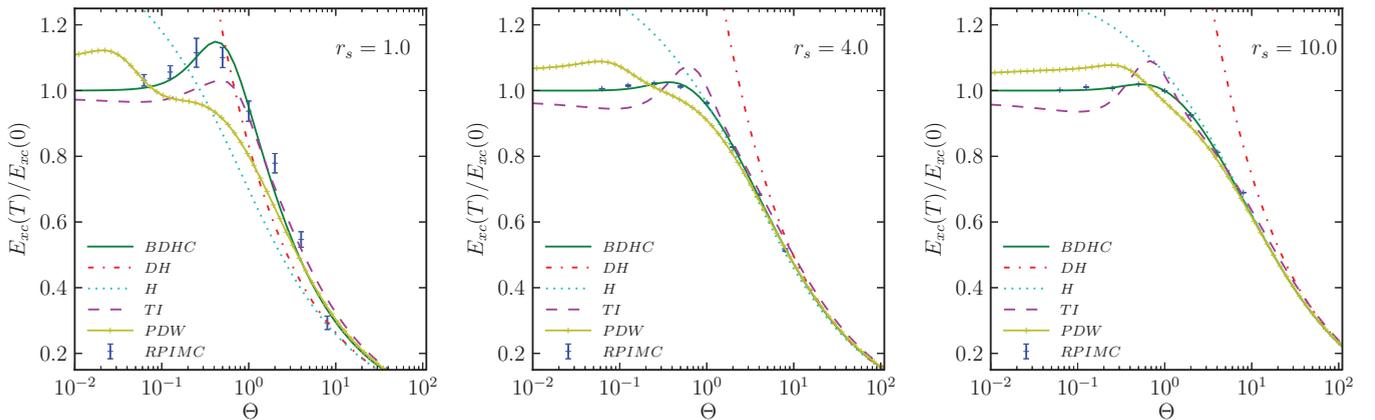
FIG. 2. (Color online) Ratio of the exchange-correlation energy E_{xc} at temperature T to that at $T = 0$ for the polarized $\xi = 1$ 3D HEG with $r_s = 1.0$, 4.0, and 10.0 (respectively). Shown are the results from numerical calculations (RPIMC), the present parametrization (BDHC), and several previous parametrizations. The latter include Debye-Hückel (DH), Hansen (H), Tanaka and Ichimaru (TI), and Perrot and Dharma-wardana (PDW), all of which are discussed in the text.

local-field corrections (LFC) through interpolation since diagrammatic resummation techniques often become intractable in strongly coupled regimes. Singwi, et al.[38] introduced one such strategy relying on two assumptions. First, they use the static polarization-potential approximation allowing one to write the LFC, $G(k,\omega) \simeq G(k,\omega = 0) \equiv G(k)$. Next they assume the two-particle distribution function is a function of the Fourier transformed momentum distribution, $n(r)$, and the pair-correlation function, $g(r)$, allowing a self-consistent solution for $G(k)$. Tanaka and Ichimaru[35] (TI) extended this method to finite temperatures and provided the parametrization of the 3D HEG correlation energy shown in Figs. 1 and 2. A similar method by Dandrea et al. uses the Vashista-Singwi LFC (Ref. 34) to interpolate between the high- and low-temperature limits. Both methods appear to perform marginally better than the RPA at all temperatures, though both still fail to produce a positive-definite $g(r)$ at values of $r_s > 2$.

A third, more recent approach introduced by Perrot and Dharma-wardana (PDW)[36] relies on a classical mapping wherein the distribution functions of a classical system at temperature T_{cf}, solved for through the hypernetted-chain equation, reproduce those for a quantum system at temperature T. In a previous work, PDW showed such a temperature T_q existed for the classical system to reproduce the correlation energy of the quantum system at $T = 0$.[39] To extend that work to finite-temperature quantum systems, they use the simple interpolation formula $T_{cf} = \sqrt{T^2 + T_q^2}$. This interpolation is clearly valid in the low-T limit where Fermi-liquid theory gives the quadratic dependence[40] of the energy on T. Further in the high-T regime, T dominates over T_q as the system becomes increasingly classical.

IV. PRESENT FIT

For our fit to RPIMC data, we employ a similar fitting functional as was used by PDW. To this end we define

$$E_{xc}(r_s,T) \equiv \frac{E_{xc}(r_s,0) - P_1}{P_2}, \qquad (1)$$

where $E_{xc}(r_s,0)$ is the ground-state exchange-correlation energy,

$$P_1 \equiv (A_2 u_1 + A_3 u_2)T^2 + A_2 u_2 T^{5/2}, \qquad (2)$$

$$P_2 \equiv 1 + A_1 T^2 + A_3 T^{5/2} + A_2 T^3, \qquad (3)$$

TABLE I. Fit parameters of the function in Eq. (6) for the unpolarized ($\xi = 0$) gas. The top three rows correspond to $r_s < 10$, while the bottom three rows correspond to $10 < r_s$.

k	a_k	b_k	c_k	d_k
1	3.56364	−2.18158	0.85073	−0.28255
2	4.97820	−2.72627	0.62562	−0.22889
3	9.41995	−3.78699	−1.87662	0.39992
1	4.38637	1.22928	−0.789404	0.178368
2	5.96304	0.249599	−0.991637	0.220769
3	5.43786	−1.10198	−0.716191	0.157061

TABLE II. Fit parameters of the function in Eq. (6) for the polarized ($\xi = 1$) gas. The top three rows correspond to $r_s < 10$, while the bottom three rows correspond to $10 < r_s$.

k	a_k	b_k	c_k	d_k
1	−1.57839	−9.99823	7.10336	−2.19297
2	−1.46754	−11.3387	7.85547	−2.40187
3	−0.784554	−11.5341	7.07407	−2.17553
1	−7.23836	19.8258	0.254584	0.0521708
2	−6.65715	19.9802	0.263629	0.0540244
3	−5.89226	17.3632	0.238536	0.0488823

$$u_1(r_s) \equiv \frac{3}{2r_s^3}, \qquad (4)$$

$$u_2(r_s) \equiv \frac{\sqrt{6}}{r_s^{3/2}}, \qquad (5)$$

and

$$A_k(r_s) \equiv \exp\left[a_k \ln r_s + b_k + c_k r_s + d_k r_s \ln r_s\right]. \qquad (6)$$

Here u_1 and u_2 are chosen such that $\lim_{T\to\infty} E_{xc}(r_s,T) = U_{DH} + U_Q + O(T^{-3/2})$. The higher-order terms reflect the higher-order quantum corrections mentioned above. Likewise, note that $\lim_{T\to 0} E_{xc}(r_s,T) = E_{xc}(r_s,0) - O(T^2)$, reproducing both the ground-state exchange-correlation energy of Ceperley-Alder[29] and the small-T quadratic behavior of Fermi-liquid theory.[41] The Perdew-Zunger[30] parametrization is used throughout for $E_{xc}(r_s,0)$. The exchange-correlation energy between this and other parametrizations is at least two orders of magnitude smaller than the difference between the lowest temperature simulated and the Perdew-Zunger result. Because of this, we expect the use of another $0T$ functional to have negligible effect on the finite-T parametrization we present.

We determine the best parameters of Eq. (6) through a least-squares fitting of RPIMC data.[42] The RPIMC data shows a qualitative change in behavior around $r_s \approx 10$ and so we divide the fitting regime into two parts, $r_s < 10$ and $r_s > 10$. At $r_s = 10$, we make sure both the functional and its derivative are continuous. This is accomplished by ensuring each factor A_k and its respective r_s derivative is continuous at $r_s = 10$, providing six constraints and leaving 18 free parameters. For the unpolarized gas $\xi = 0$, we give the parameters in Table I. Using these values, the fitting function has a maximum relative error of 0.9%. For the polarized gas $\xi = 0$, we give the parameters in Table II. Using these values, the fitting function has a maximum relative error of 0.3%. Both of these maximum deviations occur at $r_s = 1.0$ where errors from RPIMC simulation were largest. All energies are in units of Rydbergs.

V. DISCUSSION AND CONCLUSIONS

In Figs. 1 and 2, we plot our fit, the RPIMC data, and all mentioned prior fits of the finite-temperature exchange-correlation energy. Clearly, the classical Debye-Hückel limit is obeyed by each fit. However, only our fit and PDW obey the correct zero-temperature behavior [$E_{xc}(\Theta)/E_{xc}(0) \to 1$ as $\Theta \to 0$]. The Singwi-Tosi-Land-Sjölander (STLS) driven fit

of TI only agrees well with the RPIMC data at high density, i.e., where the RPA, the basis of STLS, is most applicable.

The PDW line in Figs. 1 and 2 clearly matches well with the RPIMC results in both temperature limits. It is not surprising, however, that in the intermediate temperature regime, where correlation effects are greatest, the quadratic interpolation of the temperature fails. A similar approach by Dutta and Dufty[37] uses the same classical mapping as PDW, matching the $T = 0$ pair-correlation function instead of the correlation energy. While this gives accurate results near $T = 0$, the breakdown of Fermi-liquid behavior near the Fermi temperature causes the method to overestimate the exchange hole of the pair-correlation function. A direct comparison of E_{xc} is not yet available.

Finally we note that there has been some previous work on the low-density phases of 3D HEG both at $T = 0$ (Ref. 43) and $T > 0$.[44] These include a predicted second-order transition to a partially polarized state around $r_s \simeq 50$, and a first-order transition into a Wigner crystal for $r_s > 100$. Since both these transitions are outside the range of the fit data, we do not expect to see these transitions with the above functional.

In summary, we have performed a least-squares fitting of recent RPIMC data to a functional form which reproduces both high- and low-temperature asymptotic limits exactly. This fit outperforms all previous attempts at parametrizing the exchange-correlation energy at arbitrary temperature. We are

providing a simple script of the functional in the Supplemental Material[45] as well as in Ref. 46. It is our hope that this parametrization will be useful as a basis for finite-temperature DFT functionals, and as a benchmark for orbital-free DFT studies.

Note added. Recently we have learned that another group has performed a QMC study of the zero-temperature, spin-polarized 3D HEG.[47] Nevertheless, as noted previously, our choice of the Perdew-Zunger[30] ground state exchange-correlation parameterization should have little effect on the finite-temperature functional fit we provide.

*brown122@illinois.edu

[1] W. Kohn, Rev. Mod. Phys. **71**, 1253 (1999).

[2] S. Kümmel and L. Kronik, Rev. Mod. Phys. **80**, 3 (2008).

[3] G. Chabrier, F. Douchin, and A. Y. Potekhin, J. Phys.: Condens. Matter **14**, 9133 (2002).

[4] M. Koenig, A. Benuzzi-Mounaix, A. Ravasio, T. Vinci, N. Ozaki, S. Lepape, D. Batani, G. Huser, T. Hall, D. Hicks, A. MacKinnon, P. Patel, H. S. Park, T. Boehly, M. Borghesi, S. Kar, and L. Romagnani, Plasma Phys. Controlled Fusion **47**, B441 (2005).

[5] R. Cauble, D. Bradley, P. Celliers, G. Collins, L. Da Silva, and S. Moon, Contrib. Plasma Phys. **41**, 239 (2001).

[6] N. D. Mermin, Phys. Rev. **137**, A1441 (1965).

[7] V. Karasiev and S. Trickey, Comput. Phys. Commun. **183**, 2519 (2012).

[8] T. Sjostrom, F. E. Harris, and S. B. Trickey, Phys. Rev. B **85**, 045125 (2012).

[9] S. B. Trickey, V. V. Karasiev, and A. Vela, Phys. Rev. B **84**, 075146 (2011).

[10] C. Huang and E. A. Carter, Phys. Rev. B **81**, 045206 (2010).

[11] V. V. Karasiev, T. Sjostrom, and S. B. Trickey, Phys. Rev. B **86**, 115101 (2012).

[12] L. A. Constantin, E. Fabiano, S. Laricchia, and F. Della Sala, Phys. Rev. Lett. **106**, 186406 (2011).

[13] E. W. Brown, B. K. Clark, J. L. DuBois, and D. M. Ceperley, Phys. Rev. Lett. **110**, 146405 (2013).

[14] D. M. Ceperley, Rev. Mod. Phys. **67**, 279 (1995).

[15] *Monte Carlo and Molecular Dynamics of Condensed Matter Systems*, edited by K. Binder and G. Ciccotti, Conference Proceedings Vol. 49 (Italian Physical Society, Bologna, 1996).

[16] D. M. Ceperley, J. Stat. Phys. **63**, 1237 (1991).

[17] P. Debye and E. Hückel, Phys. Z. **24**, 185 (1923).

[18] J. P. Hansen, Phys. Rev. A **8**, 3096 (1973).

[19] E. L. Pollock and J. P. Hansen, Phys. Rev. A **8**, 3110 (1973).

[20] J. P. Hansen and P. Vieillefosse, Phys. Lett. A **53**, 187 (1975).

[21] B. Jancovici, Physica A **91**, 152 (1978).

[22] A. Alastuey and A. Perez, Phys. Rev. E **53**, 5714 (1996).

[23] M. Gell-Mann and K. A. Brueckner, Phys. Rev. **106**, 364 (1957).

[24] W. J. Carr and A. A. Maradudin, Phys. Rev. **133**, A371 (1964).

[25] E. Wigner, Phys. Rev. **46**, 1002 (1934).

[26] K. Fuchs, Proc. R. Soc. London, Ser. A **151**, 585 (1935).

[27] W. J. Carr, R. A. Coldwell-Horsfall, and A. E. Fein, Phys. Rev. **124**, 747 (1961).

[28] D. Ceperley, Phys. Rev. B **18**, 3126 (1978).

[29] D. M. Ceperley and B. J. Alder, Phys. Rev. Lett. **45**, 566 (1980).

[30] J. P. Perdew and A. Zunger, Phys. Rev. B **23**, 5048 (1981).

[31] J. P. Perdew and Y. Wang, Phys. Rev. B **45**, 13244 (1992).

[32] S. H. Vosko, L. Wilk, and M. Nusair, Can. J. Phys. **58**, 1200 (1980).

[33] W. Kohn and L. J. Sham, Phys. Rev. **140**, A1133 (1965).

[34] R. G. Dandrea, N. W. Ashcroft, and A. E. Carlsson, Phys. Rev. B **34**, 2097 (1986).

[35] S. Tanaka and S. Ichimaru, J. Phys. Soc. Jpn. **55**, 2278 (1986).

[36] F. Perrot and M. W. C. Dharma-wardana, Phys. Rev. B **62**, 16536 (2000).

[37] S. Dutta and J. Dufty, Phys. Rev. E **87**, 032102 (2013).

[38] K. S. Singwi, M. P. Tosi, R. H. Land, and A. Sjölander, Phys. Rev. **176**, 589 (1968).

[39] M. W. C. Dharma-wardana and F. Perrot, Phys. Rev. Lett. **84**, 959 (2000).

[40] A. Altland and B. Simons, *Condensed Matter Field Theory* (Cambridge University Press, Cambridge, UK, 2010).

[41] Fitting exchange and correlation together avoids the canceling $T^2 \log T$ term coming from both.

[42]In fitting the data to this functional, it was noticed that the leading-order, temperature-dependent finite-size correction for the very high temperature points at small r_s was not adequate. Instead, a more useful correction for these points extends from the classical regime. Again we may write the potential energy as $V = \frac{1}{2\Omega} \sum_k \frac{4\pi q^2}{k^2} S(k)$ where the structure factor is given by $S(k) = \frac{k^2}{m\omega_p(k)} [\frac{1}{\exp^{\omega_p/T} - 1} + \frac{1}{2}]$. Here $\omega_p^2(k) \equiv \frac{4\pi n e^2}{m}(1 + k^2/k_s^2)$ with $k_s^2 \equiv 4\pi e^2/(\partial\mu/\partial n)_T$, though since we are mostly concerned with the small k limit, we take $\omega_p(k) \simeq \omega_p = 4\pi n e^2/m$. The finite-size correction then just reads as $\Delta V = V_\infty - V_N$. This correction is dominated by the long-wavelength ($k \to 0$) contribution. For $T \ll 1$ we recover the correction used in Ref. 29. For $r_s \gg T^{-2/3}$,

however, we arrive upon $\Delta V = T/(2N)$ and thus $\Delta E = T/(4N)$. Through the virial theorem we then find $\Delta K = -T/(4N)$. This new correction was applied only to the points $r_s = 1.0$, $\Theta = 4.0, 8.0$ and $r_s = 2.0$, $\Theta = 8.0$ for both the unpolarized and polarized systems.

[43]F. H. Zong, C. Lin, and D. M. Ceperley, Phys. Rev. E **66**, 036703 (2002).

[44]M. D. Jones and D. M. Ceperley, Phys. Rev. Lett. **76**, 4572 (1996).

[45]See Supplemental Material at http://link.aps.org/supplemental/10.1103/PhysRevB.88.081102 for a Fortran 90 module of the exchange-correlation functional fit and instructions for its use.

[46]http://github.com/3dheg/BDHC

[47]G. G. Spink, R. J. Needs, and N. D. Drummond, arXiv:1307.5794.